Effects of Cytochalasin D on Occluding Junctions of Intestinal Absorptive Cells: Further Evidence That the Cytoskeleton May Influence Paracellular Permeability and Junctional Charge Selectivity

James L. Madara,* David Barenberg,‡ and Susan Carlson*

Departments of *Pathology (Gastrointestinal Pathology) and ‡Medicine, Brigham and Women's Hospital; and Harvard Medical School and the Harvard Digestive Diseases Center, Boston, Massachusetts 02115

Abstract. Intestinal absorptive cells may modulate both the structure and function of occluding junctions by a cytoskeleton dependent mechanism (Madara, J. L., 1983, *J. Cell Biol.*, 97:125–136). To further examine the putative relationship between absorptive cell occluding junctions and the cytoskeleton, we assessed the effects of cytochalasin D (CD) on occluding junction function and structure in guinea pig ileum using ultrastructural and Ussing chamber techniques. Maximal decrements in transepithelial resistance and junctional charge selectivity were obtained with 10 μg/ml CD and the dose–response curves for these two functional parameters were highly similar. Analysis of simultaneous flux studies of sodium and the nonabsorbable extracellular tracer mannitol suggested that CD opened a transjunctional shunt and that this shunt could fully account for the increase in sodium permeability and thus the decrease in resistance. Structural studies including electron microscopy of detergent-extracted cytoskeletal preparations revealed that 10 μg/ml CD produced condensation of filamentous elements of the peri-junctional contractile ring and that this was associated with brush border contraction as assessed by scanning electron microscopy. Quantitative freeze–fracture studies revealed marked aberrations in absorptive cell occluding junction structure including diminished strand number, reduced strand–strand cross-linking, and failure of strands to impede the movement of intramembrane particles across them. In aggregate these studies show that CD-induced perturbation of the absorptive cell cytoskeleton results in production of a transepithelial shunt which is fully explained by a defect in the transjunctional pathway. Furthermore, substantial structural abnormalities in occluding junction structure accompany this response. Lastly, the abnormalities in occluding junction structure and function coincide with structural changes in and contraction of the peri-junctional actin-myosin ring. These data suggest that a functionally relevant association may exist between the cytoskeleton and the occluding junction of absorptive cells. We speculate that such an association may serve as a mechanism by which absorptive cells regulate paracellular transport.

THE major route for passive permeation across the mammalian ileal epithelium is paracellular (12, 25), and the rate-limiting barrier of this pathway appears to be the intercellular occluding junction (29). Furthermore, specific structural aspects of occluding junctions, such as junctional strand counts obtained from freeze–fracture replicas, appear to correlate with the ability of junctions to impede passive transjunctional flow (6, 21), particularly if variables such as linear junctional density per unit epithelial surface are fully considered (22). Recent evidence indicates that in the small intestine (20), as in gallbladder epithelium (9, 27), physiological alterations in the cellular milieu may produce major alterations in occluding junction resistance, charge selectivity, and structure. In both epithelia, the response elicited by these specific perturbations consists of expansion of occluding junction structure and restriction of paracellular ion flow with preferential restriction of paracellular cation flow. These data suggest that paracellular pathway function may be regulated by intercellular events which produce phenotypic alterations in the cell surface structure that regulates paracellular flow—the occluding junction. The cascade of intercellular events leading to such junctional modifications is presently undefined. However, in the instance of brief osmotic challenge of jejunal epithelia, the evidence suggests that the elicited intercellular "signals" may be translated into structural and functional changes in the junction by the absorptive cell cytoskeleton (20).

Elegant studies of Madin-Darby canine kidney cell mono-

layers have shown that the microfilament perturbing agent, cytochalasin B, increases passive transepithelial flow of ions, and that this is due to increased ion flow through the paracellular pathway (5, 23, 24). In natural epithelia, microfilament perturbing agents have been shown to induce alterations in occluding junction structure (1, 30), although functional assays of transepithelial permeability were either not performed or were measurements which did not specifically differentiate the paracellular from the transcellular pathway. In this study, we use cytochalasin D (CD)[1] to further probe the potential relationship between the cytoskeleton and the structure and function of occluding junctions in a natural epithelium. Using thick section, thin section, and Ussing chamber techniques, we define the effect of graded doses of CD on the structural and electrical characteristics of guinea pig ileum. Using a dual flux technique, we examine whether the effects of this agent on transepithelial electrical resistance are produced by changes in paracellular, or transcellular, permeability. Using quantitative freeze-fracture analysis, we define the effects that this agent produces on occluding junction structure. Lastly, we use detergent extraction techniques to prepare and subsequently examine cytoskeletal ghosts of tissues from these experiments.

Materials and Methods

For these experiments, 12–15-cm segments of distal ileum (excluding the final 10 cm) were obtained from Hartley-strain guinea pigs that weighed ~600–1,000 g. All animals were fasted overnight before use and were anesthetized with intraperitoneal injection of urethane.

Physiologic Techniques

Ileum was rapidly removed, opened, washed in chilled oxygenated buffer and cut into 2-cm segments. After stripping away the serosa and external longitudinal layer of the muscularis propria, these segments were mounted in modified Ussing chambers equipped with two calomel voltage-sensitive electrodes and two Ag-AgCl current passing electrodes as previously described (20). Electrodes were connected to the chamber solution via agar bridges. Both mucosal (M) and serosal (S) sides of the chamber were attached to circulating 10-ml reservoirs driven by a gas lift column of 95% O_2/5% CO_2. The reservoirs which contained the buffer described below were jacketed with a circulating water bath maintained at 37°C. The circulating buffer solution consisted of 114 mM NaCl, 5 mM KCl, 1.65 mM Na_2HPO_4, 0.3 mM NaH_2PO_4, 25 mM $NaHCO_3$, 1.25 mM $CaCl_2$, and 1.1 mM $MgSO_4$ at pH 7.4. 20 mM glucose was added to the S buffer and 20 mM mannitol was added to the M buffer for all experiments except the flux experiments as indicated below. After a 15-min equilibration period, baseline resistance was determined. Baseline tissue resistance was recorded as the absolute minus the fluid resistance. In these experiments, unless specifically stated otherwise, we optimized tissue viability by making the mucosal buffer like that described above but with the addition of the high oxygen affinity perfluorochemical, Fluosol 43 (The Green Cross Corporation, Osako, Japan). CD was obtained from Sigma Chemical Co., St. Louis, MO, solubilized in dimethyl sulfoxide, and used as a stock solution of either 1 or 2 mg CD/ml. After an experiment, the CD stock was stored at 4°C but was discarded after 1 wk if unused. In CD experiments, the final dimethyl sulfoxide concentration was 0.5%, a concentration which, in separate previous experiments (20) and in the current experiments (see Results) showed no effect on tissue resistance or structure. When used, CD was added to both reservoirs after equilibration. Final CD concentrations to which tissues were exposed ranged from 0.1 to 20 μg/ml and durations of CD exposure ranged from 20 to 60 min. Control data for the CD experiments were derived from tissue treated identically save for the exposure to CD.

Unidirectional serosal-to-mucosal solute fluxes of sodium and mannitol were determined under short-circuit conditions. After stabilization of tissues, 20 μCi [^{3}H]mannitol and 8 μCi $^{22}Na^+$ were added to the serosal reservoir. After a 10-min equilibration period, a baseline 20-min flux period was obtained. Tissues were then exposed to CD or vehicle only and two additional 20-min flux periods were analyzed. Simultaneous $^{22}Na^+$ and [^{3}H]mannitol fluxes were determined by liquid scintillation. In flux experiments, both mucosal and serosal solutions had 15 mM glucose and 5 mM cold mannitol in order to avoid a transepithelial mannitol gradient. The relationship between Na^+ and mannitol flux was analyzed by linear regression.

To assess junctional charge selectivity, 20% mucosal dilution potentials were measured as previously described (20).

Morphologic Techniques

At the end of each experiment, all tissues for routine light and electron microscopy and freeze-fracture were rapidly removed from the chambers and submerged in a 4°C solution containing 2% formaldehyde and 2.5% glutaraldehyde in 0.1 M sodium cacodylate buffer at pH 7.4. After an initial 2-h aldehyde fixation, tissues for conventional electron microscopy of thin sections were washed in 0.1 M sodium cacodylate, postfixed for 1 h in 1% osmium tetroxide, dehydrated in a graded series of alcohols, and embedded in epoxy resin. Toluidine blue-stained 1-μm sections were obtained with glass knives. Representative thin sections were mounted on copper-mesh grids and stained with uranyl acetate and lead citrate.

After fixation, tissues for freeze-fracture were washed in 0.1 M cacodylate buffer before being embedded in 3% agar and cut into 150-μm slices with a Smith-Farquhar tissue chopper. After equilibrating for 1 h in 25% glycerol in 0.1 M sodium cacodylate buffer, tissue slices were mounted between two gold discs, rapidly frozen in partially solidified Freon 22, and stored in liquid nitrogen. Specimens were fractured at a stage temperature of −110°C in a Balzers 300 freeze-etch device, replicated with platinum-carbon, cleaned in commercial bleach, and mounted on Formvar-coated 200-mesh hexagonal grids. Morphometric quantitation of absorptive cell occluding junction structure was performed as previously described (20).

For extraction of soluble cytoplasmic proteins and visualization of the cytoskeleton, sample tissues were rapidly removed from chambers and washed for 1 min in a 0.1 M phosphate buffer at pH 6.9. These were then detergent extracted by 0.1% Triton X-100 made up in a stabilization buffer which consisted of 0.1 M Pipes, pH 6.9, containing 0.2 mM phenylmethylsulfonyl fluoride, 0.2 mM dithiothreitol, 5 mM $MgCl_2$, and 5 mM EGTA. Extraction was carried out for 15 min with gentle agitation. Tissues were then briefly washed in the above stabilization buffer in the absence of Triton X-100, and fixed by transferring them for 30 min to a 0.1-M phosphate buffer solution, pH 6.9, containing 1% glutaraldehyde and 0.2% tannic acid. After a phosphate buffer wash, tissues were postfixed on ice in a 0.1-M phosphate buffer solution containing 0.5% osmium tetroxide, at pH 6.0 for 30 min. After another rinse in phosphate buffer, tissues were block stained for 45 min in a 1% aqueous uranyl acetate solution before being dehydrated and embedded by routine techniques.

Scanning electron microscopy of the villus surface was performed as previously described (22).

Results

Functional Effects of CD

After the initial period of equilibration, ileal epithelium mounted in chambers maintained a stable transepithelial resistance for 60 min (Fig. 1). In contrast, when exposed to 10 μg/ml CD for 60 min, transepithelial resistance declined to values approximately one half that of the initial reading (Fig. 1). The major resistance decline occurred between 10 and 40 min after CD exposure (Fig. 1). Exposure of mucosal sheets to varying doses of CD for 60 min showed that a decrement in resistance could not be detected at doses <1 μg/ml and that the maximal effect occurred at a dose of 10 μg/ml (Fig. 2). The ability of occluding junctions to preferentially impede anion over cation permeation, as judged by 20% mucosal dilution potentials,[2] also decreased to ~50% of con-

1. *Abbreviation used in this paper:* CD, cytochalasin D.

2. To measure dilution potentials, we diluted mucosal Na and Cl concentrations without creating an osmotic gradient across the epithelium (20). Thus, Na and Cl are driven down their activity gradients across the occluding junction. If the junction is charge selective, an electrical potential will be generated, and the size of this potential (in mV) represents a measurement of the degree of junctional charge selectivity. The polarity of the potential will differentiate cation from anion selectivity.

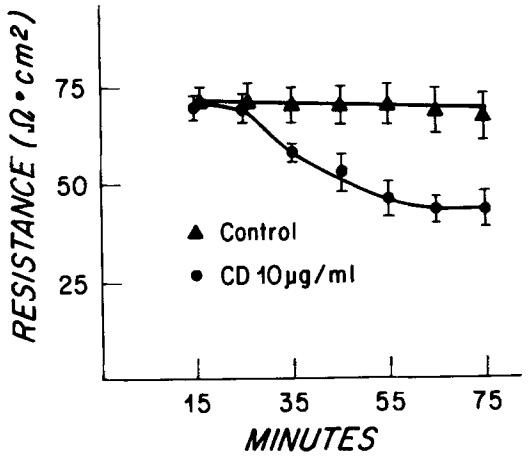

Figure 1. Time–course of transepithelial resistance response of guinea pig ileal epithelium after exposure to 10 μg/ml CD. CD was added after a 15-min equilibration period. The major resistance decrement occurs in the first 40 min after exposure.

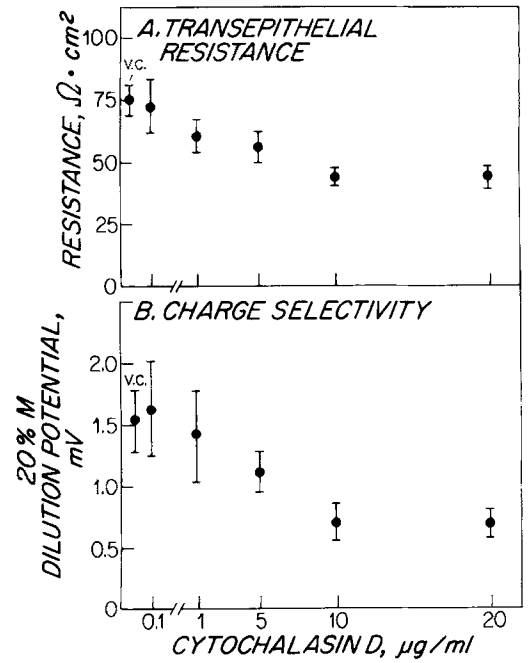

Figure 2. Effect of graded doses of CD on transepithelial resistance and on junctional charge selectivity. The dose–response curve obtained for resistance closely parallels that for charge selectivity (here, cation selectivity, since the data are expressed as mucosal solution positive). *v.c.*, vehicle control.

trol values after 60-min exposure to 10 μg/ml CD (Fig. 2). Furthermore, the dose–response curve obtained for dilution potentials closely paralleled the dose–response obtained for transepithelial resistance (Fig. 2). Unidirectional fluxes of mannitol, an extracellular marker (8) which has a hydrodynamic radius small enough (3.6 Å) to permeate occluding junctions in native (11) and in cultured intestinal epithelia (21), were also altered by CD exposure. In equilibrated control tissues, the mean serosal-to-mucosal mannitol flux in the first 20-min flux period was 6.0 $\mu M/cm^2 \cdot h \times 10^{-2}$ (Fig. 3). After addition of the vehicle only, the two subsequent flux periods showed comparable rates of mannitol flux. In contrast, in the

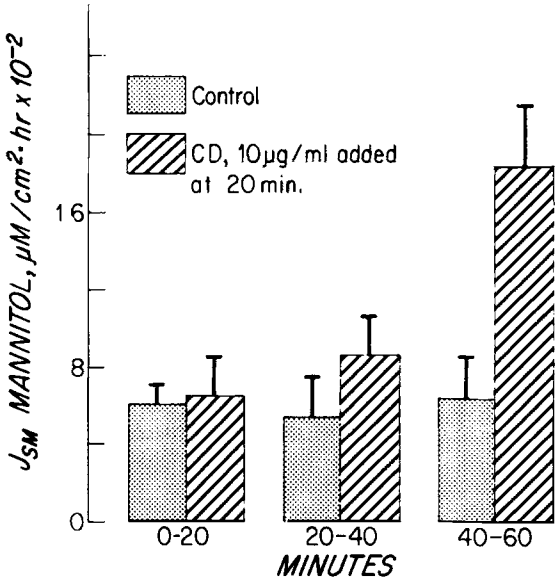

Figure 3. Serosal to mucosal flux rates of the extracellular space marker mannitol in control tissues and in tissues treated with CD. CD was added after the first 20-min flux period. Thus the striped bar at 0–20 min represents the baseline flux rate of tissues which were subsequently exposed to CD while the dotted bar at this time interval represents the flux rate of tissues which subsequently were exposed to vehicle only. Mannitol flux is modestly increased in the 20 min after CD exposure, but is greatly increased in the subsequent 20-min flux period. In control tissues exposed to vehicle alone, flux rates are comparable for the three flux periods.

two 20-min flux periods after exposure to 10 μg/ml CD, mean mannitol flux was ~9.0 $\mu M/cm^2 \cdot h \times 10^{-2}$ and 19.0 $\mu M/cm^2 \cdot h \times 10^{-2}$, respectively (Fig. 3). Likewise, mean baseline serosal-to-mucosal sodium flux (9.8 $\mu Eq/cm^2 \cdot h$) was not affected by the addition of the vehicle but sequentially increased in the two flux periods after the addition of 10 μg/ml CD (11.5 and 15.4 $\mu Eq/cm^2 \cdot h$, respectively).

We next assessed if the CD-induced increment in paracellular permeability as indicated by the increment in mannitol flux could fully explain the increment in sodium flux, and thus the CD-elicited decrease in resistance. If the increment in sodium flux was wholly related to the CD-induced, mannitol-permeable pathway, then the following statement would hold: the slope of the relationship plotting sodium flux against mannitol flux for all experiments would not be larger than the ratio of the free solution diffusion coefficients of these two molecules corrected for the concentrations of each present in the bath (8, 11). In other words, we are asking if the increase in mannitol-permeable space fully accounted for the observed increase in tissue permeability to ions. If so, since resistance measurements are measurements of tissue ion permeability, the data would indicate that the increment in paracellular mannitol permeation fully explained the alterations in tissue resistance. Thus, the effect of CD on tissue permeability would be entirely due to the effect of this agent on paracellular permeability. If the pathway responsible for increased mannitol permeability was also responsible for the increase in sodium permeability, the slope of the relationship in Fig. 4 should be no greater than $D^{Na} \cdot 140\ mM/D^{man} \cdot 5\ mM$, where D is the free solution diffusion coefficient for each molecule at 37°C ($1.78 \pm 10^{-5}\ cm^2 \cdot s^{-1}$ for sodium [31], 0.92×10^{-5}

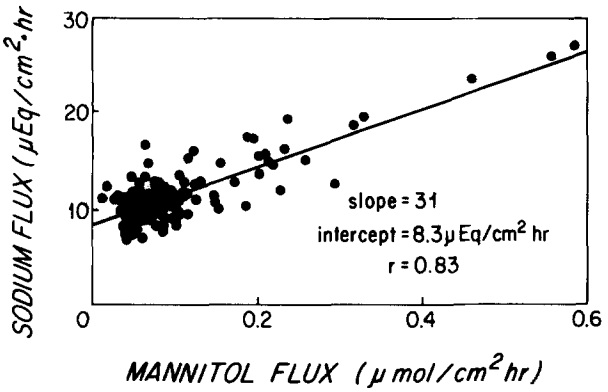

Figure 4. Correlation between serosal-to-mucosal sodium and mannitol fluxes as determined simultaneously using dual flux techniques. This graph, which plots all periods of CD-exposed and non-exposed control tissues, shows that the mannitol-permeable pathway (paracellular) induced by CD exposure fully accounts for the increment in Na^+ flux, and therefore the decrement in resistance produced by this agent (see Discussion).

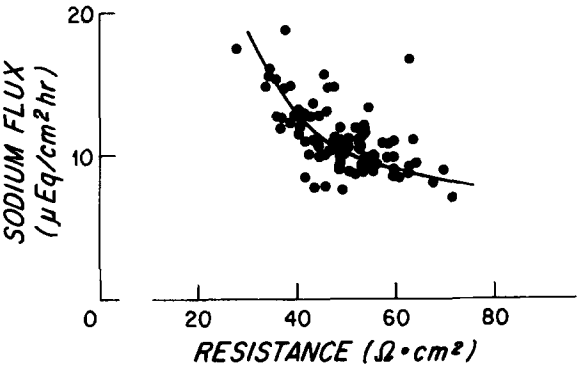

Figure 5. The relationship between transepithelial resistance and sodium flux for control and CD-treated epithelia. These parameters of permeability correlate in an asymptotic fashion.

$cm^2 \cdot s^{-1}$ for mannitol [18]). The value for this predicted slope is 54. The actual slope of the relationship in Fig. 4 is 31, indicating that the induced mannitol pathway fully accounts for the increment in sodium flux. Sodium and mannitol fluxes were also highly correlated ($r = 0.83$) with one another (Fig. 4) and the intercept of this relationship was substantially different than 0 (8.3 μEq $Na^+/cm^2 \cdot h$).

The simultaneous flux experiments from which the above data were derived were performed with the presence of the oxygen carrying fluorocarbon, Fluosol, on the mucosal side. To be certain that presence of Fluosol did not affect these results, we repeated the experiment (control, $n = 8$; CD, $n = 8$) with buffer only in the serosal and mucosal compartments. The correlation ($r = 0.92$), slope (33), and intercept (8.1 μEq $Na^+/cm^2 \cdot h$) obtained under these conditions were comparable to those above.

The relationships between resistance and the serosal to mucosal fluxes of Na^+ (Fig. 5) and mannitol (Fig. 6) appeared to be asymptotic. Such data highlight the sensitivity of resistance measurements for detecting small changes in paracellular permeability (see reference 21 for explanation of this phenomenon based on analysis of electrical circuits). As minor populations of conductive sites are introduced into the epithelium, resistance falls substantially, but mannitol flux increases

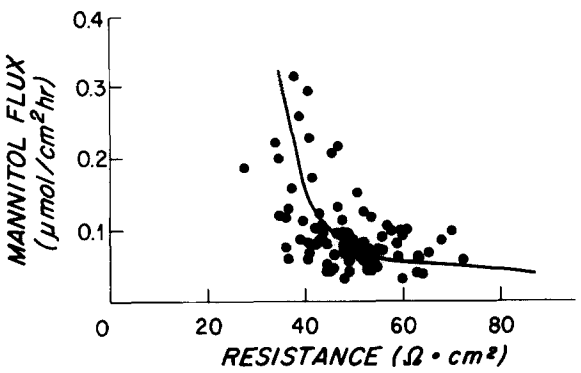

Figure 6. The relationship between transepithelial resistance and mannitol flux for control and CD-treated epithelia. These parameters of permeability correlate in an asymptotic fashion.

are very minor. Since resistance values can be dominated by a minor population of permeable sites (21), further expansion of the number of permeable sites does little to further decrease resistance. However, as high permeability sites become more numerous, this major increase in conductive sites is readily detected by mannitol flux—a type of data which reflects mean function of permeability sites. Thus when one plots the resistance readings against the flux readings of tissues progressively perturbed by CD, asymptotic relationships are observed.

Structural Effects of CD Relevant to Paracellular Pathway

Control tissue mounted in chambers for periods of up to 100 min revealed an intact ileal epithelium with villi lined predominantly by columnar absorptive cells displaying a lush microvillus brush border, with occasional extruding cells lying over the upper portion of the villus (Fig. 7). This morphology varies from that in the fasted, intact animal only in that villi are somewhat shorter (due to the absence of an intact muscularis propria), and villus tip paracellular spaces are occasionally somewhat more open (due to solute and water absorption in the absence of a functioning capillary circulation). Short-term exposure (30–40 min) to CD, 10 μg/ml, produced several alterations in mucosal structure (Fig. 8) which were confined to the absorptive cells on the upper one half of the villus. The most striking result was the appearance of a markedly serrated apical border, produced by rounding of absorptive cell apices (Fig. 8). Initially, tissues exposed to 10 μg/ml CD were examined after four durations of exposure: 15, 30, 40, and 60 min. The above structural effects were inapparent at 15 min and became more readily apparent with time, and relatively uniform at 30 and 40 min. The structural effects produced by 10 μg/ml CD varied a great deal in severity from tissue to tissue after a 60-min exposure, however. Tissues exposed for 60 min, while often structurally similar to those described above, occasionally displayed striking villus absorptive cell extrusion associated with marked villus border serration. For this reason, and since ~70–80% of the functional effect of CD was achieved by 40 min (Fig. 1), we limited our subsequent flux studies to tissues exposed to CD for 30–40 min.

As judged by thin section, absorptive cells on the upper half of the villus also displayed structural abnormalities of the

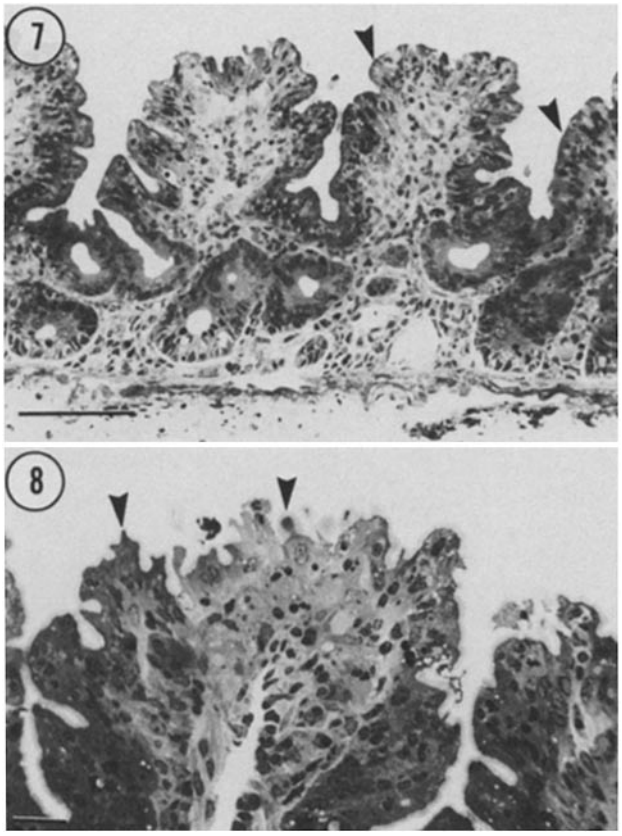

Figures 7 and 8. Light micrographs of guinea pig ileal mucosa mounted for 60 min in an Ussing chamber. (Fig. 7) Control preparation mounted for 20 min and subsequently exposed to vehicle for 40 min. The epithelium is intact and the apical border composed of absorptive cell brush borders is smooth (arrowheads). Bar, 100 μm. (Fig. 8) Preparation mounted for 20 min and subsequently exposed to 10 μg/ml CD for 40 min, demonstrating extreme example of morphological alteration. While the epithelium is intact, the apical border of the villus epithelium is serrated. The serration of the villus border induced by CD is produced by apparent rounding of the superficial portions of villus absorptive cells (arrowheads), some of which produce protuberances which jut into the lumen. Bar, 20 μm.

terminal web after 30–40 min of exposure to 10 μg/ml CD. Rather than having the typical uniform band of densely intermeshed microfilaments underlying the microvillus border, spherical aggregates of filaments separated by zones relatively devoid of terminal web cytoskeletal elements were seen (Fig. 9). In these latter areas of terminal web discontinuity, cytoplasmic organelles such as endoplasmic reticulum and mitochondria, which are usually excluded from the terminal web zone (Fig. 10) (34), closely approached the apical membrane (Fig. 9). A preferential site for condensation of terminal web cytoskeletal components was at the perijunctional zone (Fig. 9). Multifocally, at perijunctional sites the apical membrane was elevated to a "peak" at the site of the occluding junction, and perijunctional microvilli were lost.

The distribution of terminal web cytoskeletal elements was more clearly outlined in detergent-extracted preparations. In control tissues and in tissues exposed to concentrations of CD which did not elicit a decrease in resistance, the terminal web consisted of a uniform web of cytoskeletal elements extending as a continuous band across the apical cytoplasm of absorptive cells (Fig. 11). The depth of the terminal web was ~0.5–0.8 μm in control tissues and the density of this zone appeared uniform across individual absorptive cells. In contrast, tissues exposed to 10 μg/ml CD for 40–60 min often displayed great irregularity in the terminal web of absorptive cells located on the upper portion of the villus. Terminal web thickness was irregularly decreased in these tissues and condensations of cytoskeletal elements, most marked in perijunctional areas, were observed (Fig. 12). Such perijunctional condensations most frequently were in direct apposition with the junctional complex membrane (Fig. 12). As seen in unextracted CD-exposed tissues, but not in controls, cytoskeletal condensations were also occasionally scattered throughout the terminal web zone, even in areas removed from the junction. Sections cut in a plane roughly parallel to the cell surface and at the level of the junctional complex showed that the lateral membrane at the level of the junctional complex has associated with it on the cytoplasmic side a fine, often indistinct, band of microfilaments (Fig. 13) which ring the apex of the cell. In contrast, CD treatment elicited condensation of the cytoskeletal elements within this ring (Figs. 14 and 15). This feature took the appearance of multifocal, dense, and irregular condensation of the microfilaments of this ring zone. Such alterations were multifocally present within 40 min of exposure to 10 μg/ml CD, but were striking and widely distributed by 60 min. This effect of CD on perijunctional structure was exaggerated at three cell junctions (Figs. 14 and 15).

Scanning electron micrographs of vehicle control tissues revealed villus ridges which displayed relatively smooth surface contours (Fig. 16) due to the smooth, flat apical surface of villus absorptive cells that lined them (Fig. 17). In contrast, CD-exposed tissues showed rough cobblestone-like villus surfaces (Fig. 18) due to convexity of absorptive cell surfaces (Fig. 19). Such convexities were associated with flaring of microvilli as if the neck of cells had been constricted in a purse-string fashion (Fig. 19).

Freeze–fracture images of control tissues revealed absorptive cell occluding junctions which appeared as a uniform band of four to six intermeshed P face strands or E face grooves (Fig. 20). Although many similar junctional images were observed in tissues exposed to 10 μg/ml CD for 30–40 min, these later tissues had a structural subset of absorptive cell occluding junctions not seen in control tissues. Such junctions frequently occurred in areas in which the density of microvilli was diminished and thus presumably corresponded to foci which, by thin section, displayed perijunctional cytoskeletal condensations with associated loss of perijunctional microvilli (Fig. 21). Occluding junctions in these areas consisted of an irregular array of strands or grooves. In such areas, lateral membrane P face intramembrane particles which were excluded from the interstrand areas of control occluding junctions (Fig. 20) often penetrated the incompletely isolated interstrand spaces (Fig. 21). Such junctional areas often contained sites at which a deformed apical membrane jutted into the lumen—a feature corresponding to the apical membrane "peaks" which were noted in thin sections and were seen overlying sites that displayed perijunctional cytoskeletal condensations. In some such extremely aberrant junctions, the distortion of the apical membrane produced irregular fracture planes, which partially obscured apical junctional stands and, thus, interfered with quantitative assays of strand counts.

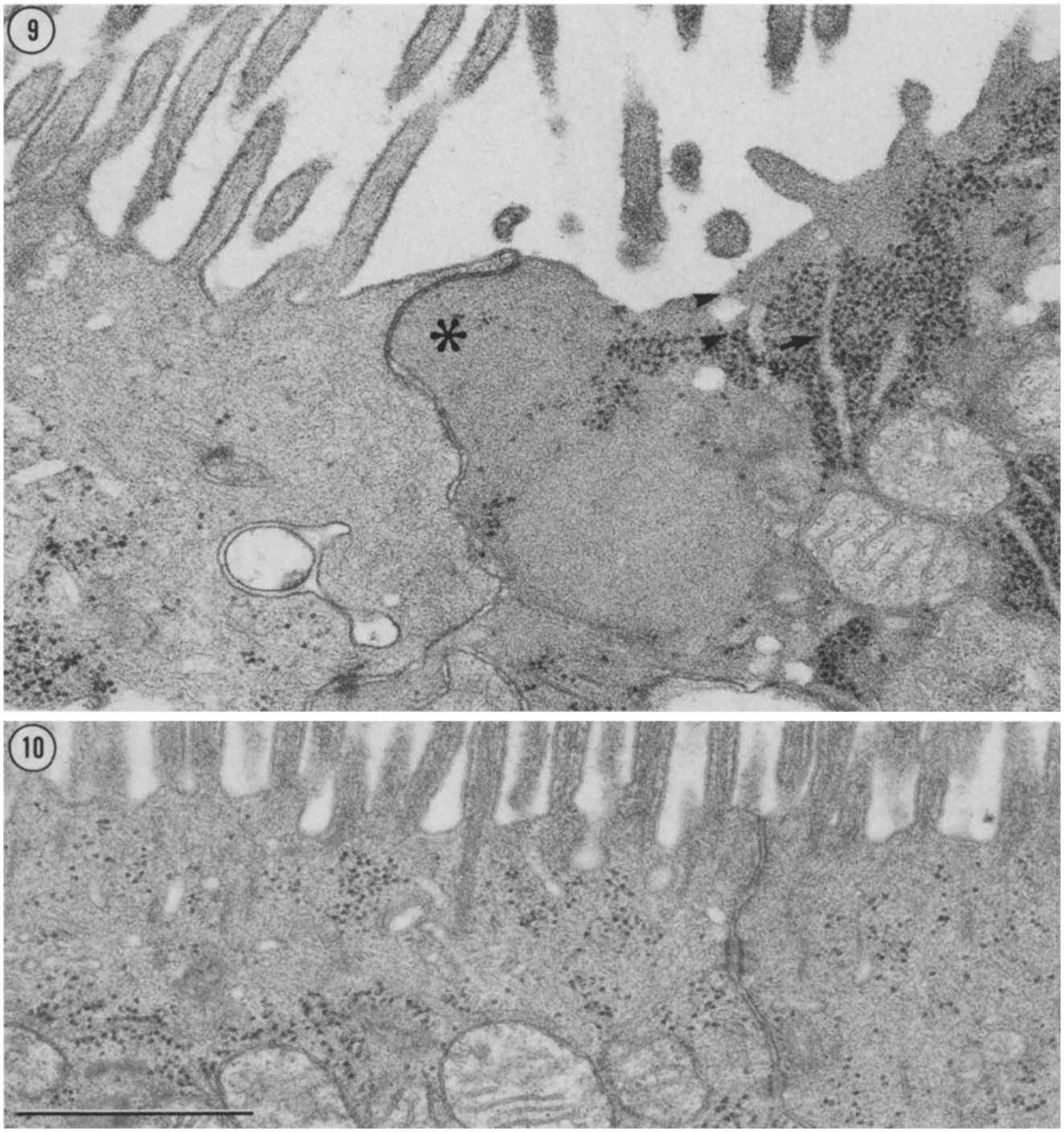

Figures 9 and 10. Electron micrographs of villus absorptive cells exposed 40 min either to vehicle (Fig. 10) or to 10 μg/ml CD (Fig. 9). The cell on the right of Fig. 9 displays a highly condensed aggregate of structural components of the terminal web which are located in a peri-junctional position (asterisk). The remainder of the terminal web present in this view is thinned (arrowheads) and organelles usually restricted from this area approach the apical membrane (arrow). Peri-junctional microvilli have been lost from both cells. In contrast, the depth of the terminal web is uniform in control tissues (Fig. 10) and peri-junctional microvilli have not been lost. Bar, 1 μm.

Thus, strand counts given below should underestimate the junctional abnormalities elicited by CD. Other abnormalities in absorptive cell occluding junction structure elicited by CD included loss of strand–strand cross-linking and focal total discontinuity (Fig. 22). Analysis of replicas that contained areas of oriented villi revealed that such abnormalities in absorptive cell occluding junction structure were largely localized to the upper portion of the villus.

Histograms of absorptive cell occluding junction strand count, a structural parameter which often appears to relate to junctional resistance (6, 20, 21), demonstrated that junctions of tissues exposed to 10 μg/ml CD for either 30 or 60 min had strand counts of three or less at a much higher frequency than did junctions of controls (Fig. 23).

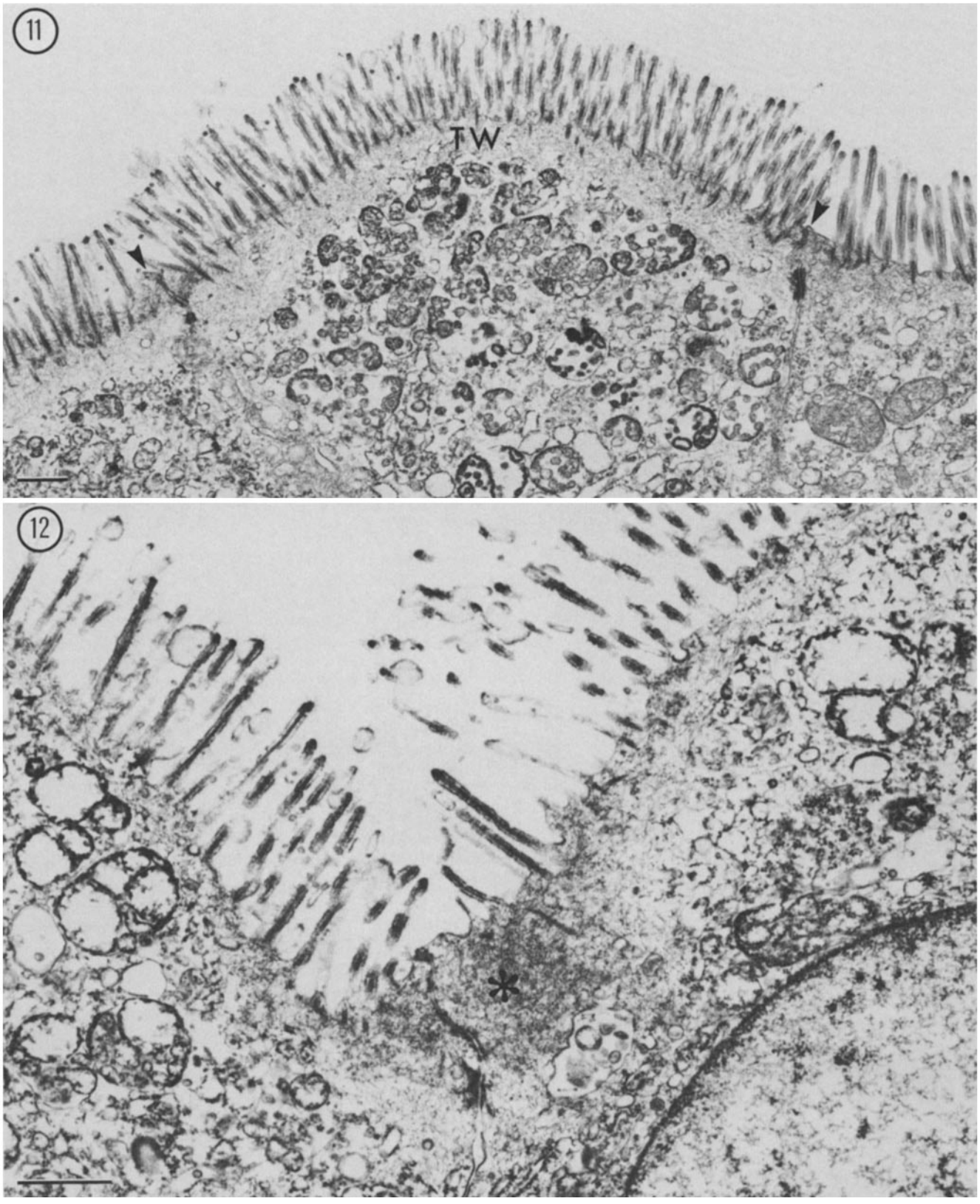

Figures 11 and 12. (Fig. 11) Transmission electron micrograph of Triton X-100–extracted villus absorptive cells exposed to vehicle alone for 40 min. The terminal web (*TW*) is of uniform density and is not appreciably augmented at junctional zones (arrowheads). Bar, 1 μm. (Fig. 12) Transmission electron micrograph of Triton X-100–extracted villus absorptive cells exposed to 10 μg/ml CD for 40 min. Filaments composing the terminal web are not matted into a zone of uniform depth and are preferentially condensed in the peri-junctional zone (asterisk). Bar, 1 μm.

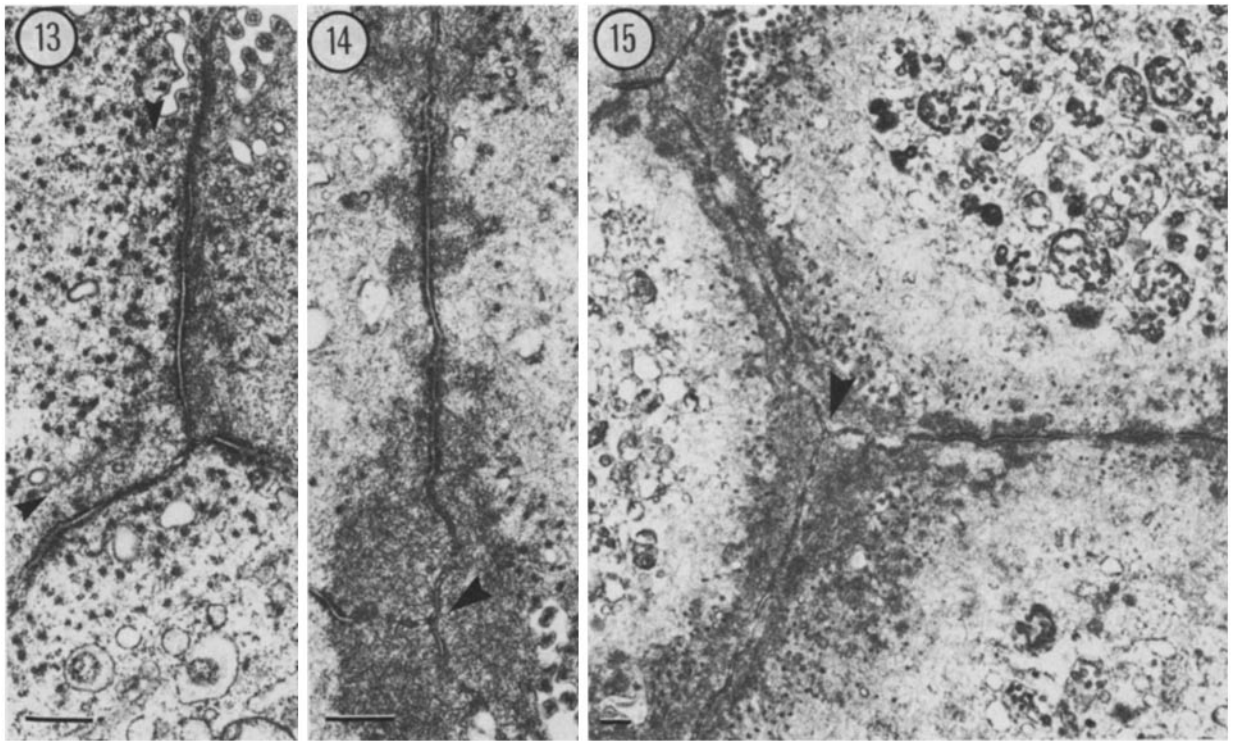

Figures 13–15. Electron micrographs of Triton X-100–extracted control (vehicle, 60 min, Fig. 13) and CD-exposed (10 μg/ml, 60 min, Fig. 14) mucosal sheets sectioned at the level of the junctional complex in planes roughly parallel to the apical surface. Control (Fig. 13) cells show a thin ring-link belt of microfilaments that run parallel to the lateral membrane (arrowheads). In marked contrast, CD exposure (Figs. 14 and 15) elicits dense irregular condensation of microfilaments in the zone of this ring which may be exaggerated where three cells meet (arrowheads) (Figs. 14 and 15). Bars, 1 μm.

Discussion

Previous studies have shown that, at least in the Madin-Darby canine kidney cell line, cytochalasins decrease transepithelial resistance and that this effect is predominantly a paracellular one as suggested by microelectrode surface scanning studies (5, 23, 24). However, parallel quantitative studies of occluding junction structure were not performed. Studies performed in native epithelia such as Necturus gallbladder (1) and rat liver (30) have demonstrated structural effects on occluding junctions elicited by cytochalasins which included disorganization of strands. Although net transepithelial resistance alterations (which, depending on dose, varied in direction of change) were recorded in one of these studies (1), data which could distinguish paracellular from transcellular function were not obtained. Given the suggestion that paracellular transport might be actively regulated and that, in the intestine, one mechanism by which such regulations might be ultimately expressed is by cytoskeletal-mediated manipulation of occluding junction structure (20), we examined, in detail, the structure and function of the occluding junction after cytoskeletal perturbation induced by CD.

We show that transepithelial resistance of guinea pig ileal mucosa may be decreased by exposure to CD. Transepithelial flux measurements of the intestinal paracellular space marker mannitol (8) revealed that the decrease in resistance coincided with an increase in mannitol flux and therefore, paracellular permeability. Identification of the paracellular pathway as the sole or at least predominant site of the CD-induced resistance decrease is problematic in an epithelium as geometrically complex as the small intestine. The irregular surface contour of this epithelium would preclude microelectrode surface scanning studies such as those which have been used in monolayers to localize paracellular current sinks (24). To ascertain if at least the major fraction of the increased permeability to ions as measured by resistance recordings represented ion permeation through the extracellular, mannitol-permeable channel induced by CD, we used the approach of Dawson (8) in which one simultaneously measures serosal to mucosal mannitol and Na^+ fluxes. Based on the concentration of the two molecules used and their relative diffusion coefficients, one can assess if the increment in the mannitol-permeable (paracellular) pathway fully accounts for the increment in passive ion permeability as judged by Na^+ flux, and therefore the decrease in resistance (8). A similar approach was used by Freel et al. (11) to pinpoint the paracellular pathway as the site at which intestinal passive permeability is increased after exposure to the dihydroxy bile salt taurochenodeoxycholate (11). We found that the mannitol-permeable channel (i.e., the paracellular channel) fully accounted for the increase in passive ion flow across this epithelium. Structural studies which showed that ileal epithelium was intact at times when paracellular permeability was enhanced rule out the possibility that the functional responses measured merely represented transepithelial holes produced by necrosis of epithelial cells. Rather, these studies indicate that the functional response is attributable to selective perturbation of paracellular as opposed to the transcellular pathway. Since the occluding junction represents the rate-limiting barrier to passive

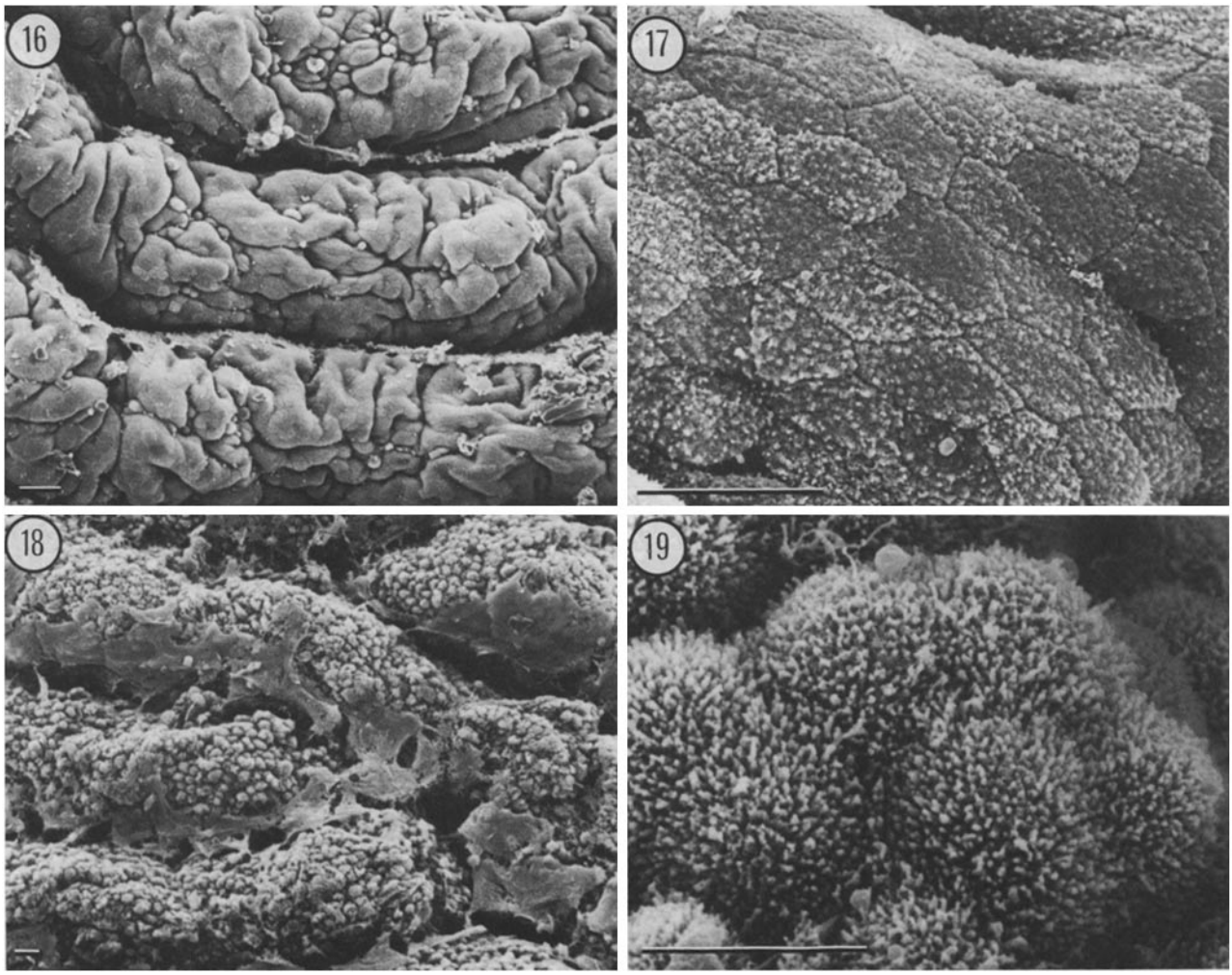

Figures 16–19. Scanning electron micrographs of vehicle control (Figs. 16 and 17) and CD-exposed (Figs. 18 and 19) (10 μg/ml, 60 min) mucosal sheets. The three villus ridges (Fig. 16) display smooth surfaces with intermittent linear folds. As seen in Fig. 17, control villi are covered by polygonal absorptive cells with flat apical surfaces. In contrast, CD-exposed tissues display a cobblestone-like appearance of the villus surfaces (Fig. 18). Higher magnification (Fig. 19) shows this cobblestone effect is due to purse-string contraction of the brush borders of individual absorptive cells resulting in a convex apical absorptive cell surface and flaring of microvilli. Bars, 20 μm.

paracellular permeability (29), this is the site at which CD would logically be assumed to be altering passive permeation of ileal epithelium. Furthermore, since the dominant effect on general cellular structure elicited by CD occurred in villus absorptive cells, it is likely that the observed increase in occluding junction permeability occurs at this specific site within the epithelium. The notion that perturbation in absorptive cell occluding junction function served as the basis for the increased permeability elicited by CD was further supported by findings derived from our freeze–fracture studies. After CD exposure many absorptive cells displayed either structurally perturbed occluding junctions or junctions composed of relatively few strands. Since occluding junction strands appear to represent the site of the resistive barrier to passive ion flow (6, 21, 22, 29), a decrease in transepithelial resistance due to an increase in paracellular conductance would be expected and was observed. Given these gross distortions in occluding junction structure, it is not surprising that, as indicated by dilution potentials, the ability of occluding junctions to discriminate between cations and ions was also grossly impaired. Since CD-induced cytoskeletal disruption may effect many intracellular processes, we cannot be certain of the exact intracellular events responsible for the observed structural and functional alterations in absorptive cell occluding junctions.

Our results with the dual flux studies allow us to offer additional speculation relating to the nature of the permeable sites ("pores") within the occluding junction strands. This relationship did not pass through the origin but rather had an Na^+ axis intercept substantially different than 0. Furthermore, the Na^+ intercept is ~80% of the value of the Na^+ flux rate across tissues unexposed to CD (9.8 $\mu Eq/h \cdot cm^2$), and it is known that, in this epithelium, the majority of the passive Na^+ flux takes a transjunctional route (12). Thus, these data suggest that only a small subpopulation of normal junctional pores permeable to Na^+ are also permeable to mannitol. Thus, junctional pores may be somewhat heterogeneous in size with the major population restricting permeation by molecules with hydrodynamic radii of 3.6 Å or greater. A second observation that the increment of CD-elicited Na^+ flux is less than

Figures 20 and 21. Freeze–fracture replicas of villus absorptive cell occluding junctions. (Fig. 20) Control junctions are composed of a net-like mesh of cross-linked strands or grooves. Peri-junctional microvilli are densely aligned above the junction. Bar, 0.1 μm. (Shadow angle, approximately left to right.) (Fig. 21) Junction exposed to 10 μg/ml CD for 40 min. Junction is composed of an irregular array of strands that underlie occasional broad protrusions of the apical membrane (arrowheads). Geometric irregularities produced by such protrusions result in a fracture plane which only focally includes the apical-most strand (straight arrows). Many peri-junctional microvilli are lost and intramembrane particles penetrate into the incompletely isolated intrajunctional compartments (curved arrow). Bars, 0.1 μm. (Shadow angle, approximately left to right.)

expected (given the size of the increment in mannitol flux) is also of interest. If CD exposure resulted in the introduction of a series of "new" hydrophilic channels permeable to mannitol, then obviously these channels would be permeable to Na^+ given the relative sizes of the hydrated radii of these

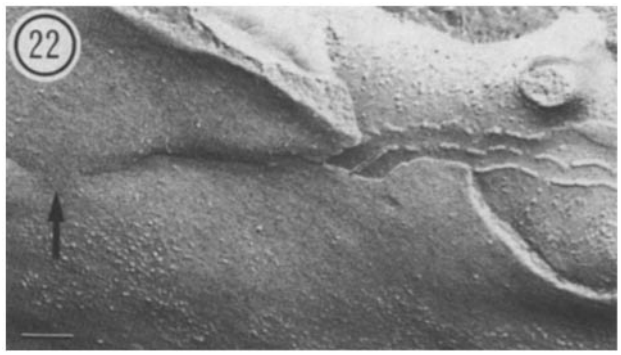

Figure 22. Freeze–fracture replica of absorptive cell occluding junction from epithelial sheet exposed in vitro to CD (10 μg/ml) for 40 min. Parallel strands deficient in cross-linking are present on the P face as is a focal trans-junctional discontinuity on the E face (arrow). Peri-junctional microvilli are diminished in number at this junctional site, corresponding to the thin section images in areas of perijunctional cytoskeletal plaques. Bar, 0.1 μm. (Shadow angle, approximately left to right.)

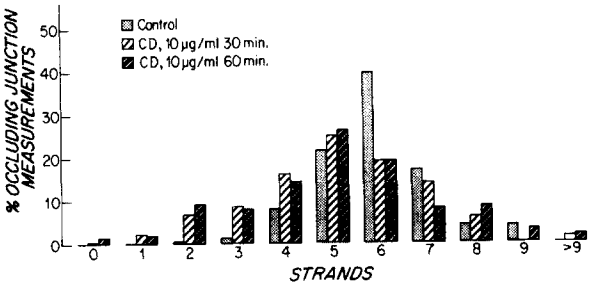

Figure 23. Histogram of absorptive cell occluding junction strand counts from control epithelial sheets and from epithelial sheets exposed to 10 μg/ml CD for 30 or 60 min. CD exposure results in an increased frequency of occluding junctions having few strands.

molecules. One interpretation of the observed data is that CD alters the conformation of some junctional pores without substantially altering their cross-sectional area, and this speculative conformational change permits mannitol permeability.

We have previously suggested that, due to the nature of the transepithelial resistance measurement, relatively minor alterations in junctional permeability would produce substantial alterations in resistance (22). Thus the initial introduction of a small subpopulation of permeable junctions might lower resistance before obvious alterations were detected in mean parameters of junctional permeability, such as flux measurements. The current data which show asymptotic relationships between resistance and flux measurements of permeability support this view. Thus, trivial increments in mannitol or Na^+ permeability are associated with rapidly falling resistances. As mannitol- and Na^+-permeable pathways begin to appear at higher frequency, major alterations in flux rates occur but are paired with more minor alterations in resistance. Thus, while flux data represent an averaged functional assay of permeability, resistance data are skewed toward the function of minor populations of pathways with low resistance to passive flow.

In addition to altering occluding junction structure and function, CD elicited the appearance of aggregated cytoskel-

etal elements in the perijunctional zone. This is the site at which a dense circumferential ring of actin (13) and myosin (13) exists both in intestinal (13, 15) and in many other epithelia (14, 26). Although the major site at which elements of this ring associate with the lateral membrane is at the level of the intermediate junction (13), a minor association between this ring and the lateral membrane at the level of the occluding junction appears also to exist in at least some epithelia (14). In permeabilized epithelia, ATP elicits contraction of this ring (4, 13, 16, 17, 32) by a process which is dependent on the presence of myosin (4) and on phosphorylation of myosin light chain (16, 17). The CD-elicited cytoskeletal plaques may represent contraction of segments of this ring. Schilwa (33) observed similar plaques of filamentous material following exposure of cultured green monkey kidney cells to CD. Based on stereo imaging data and on analysis of material released from the cytoskeleton by CD, he concluded that such plaques represent contraction of cytoskeletal segments isolated from one another after random multifocal disruption of actin microfilaments (33). Other studies suggest that cytochalasins may affect actin gels by inhibiting actin filament interaction with other actin filaments (19) or by inhibiting actin polymerization (3, 10, 19). Recent observations indicate that, although cytochalasin B may effect actin polymerization in vitro by slowing monomer addition to the barbed end of microfilaments, it also induces actin filament fragility (2). As a result of this fragility, gentle shear forces may result in severing of actin microfilaments (2). It is possible that the absorptive cell contractile ring normally experiences gentle shear forces. Such forces could result from tension intrinsic to the ring or from the flow of lumenal content over the cell surface. Superimposed cytochalasin-induced actin filament fragility might result in microfilament severing under these conditions and thus a reduction in actin filament length. Subsequent interaction of "fractured" fragments with myosin could result in contractile condensation of these elements. This latter suggestion is based on recent observations obtained from purified actin preparations in which it was noted that modest reductions of actin filament length generated an enhancement of actomyosin ATPase activity (7). Such a sequence would fit our observations, and would also account for the CD-elicited actin fragment release from cytoskeletal preparations observed by Schliwa (33). Furthermore, contraction of elements of the peri-junctional actin-myosin ring might well increase the tension on the lateral membrane at the site of the junctional complex since, as noted above, elements of this ring appear to associate with the lateral membrane at this site. Mechanical tension has been reported to produce structural rearrangement of occluding junctions in other epithelia (28) and, in general, occluding junction structure and permeability are closely linked (5, 6, 9, 20–24, 27). We speculate that the tensile state of this ring in intestinal absorptive cells may influence occluding junction structure and thereby may exert effects on and potentially regulate transepithelial permeability and paracellular transport in intact intestinal epithelium.

We thank Drs. Edward Bonder and David Begg (Department of Anatomy and Cellular Biology, Harvard Medical School) for helpful discussions and critical comments. We also thank Dr. Bonder for providing us with a manuscript of his work performed in collaboration with Dr. Mark Mooseker (Department of Biology, Yale University), before it appeared in press. We thank Ms. Mary LoGiudice and Ms. Nancy Babine for their efforts in preparation of this manuscript, and Ms. Dianna Picton for her technical expertise in preparing the detergent extracted and scanning electron microscopic specimens.

This work was supported by grants AM35932 and AM07121 from the National Institutes of Health. Dr. Madara is supported, in part, by the American Gastroenterological Association/Ross Research Scholar Award.

Received for publication 17 August 1985, and in revised form 10 February 1986.

References

1. Bentzel, C. H., B. Hainau, S. Ho, S. W. Hui, A. Edelman, T. Anagnostopoulos, and E. L. Beneditt. 1980. Cytoplasmic regulation of tight junction permeability: effect of plant cytokinins. *Am. J. Physiol.* 239:C75–C89.

2. Bonder, E. M., and M. S. Mooseker. 1986. Cytochalasin B slows but does not prevent monomer addition at the barbed end of the actin filament. *J. Cell Biol.* 102:282–288.

3. Brenner, S. L., and E. D. Korn. 1979. Substoichiometric concentrations of cytochalasin D inhibit actin polymerization. *J. Biol. Chem.* 254:9982–9985.

4. Burgess, D. R. 1982. Reactivation of intestinal epithelial brush border motility: ATP-dependent contraction via a terminal web contractile ring. *J. Cell Biol.* 95:853–863.

5. Cereijido, M., I. Meza, and A. Martinez-Palomo. 1981. Occluding junctions in cultured epithelial monolayers. *Am. J. Physiol.* 240:C96–C102.

6. Claude, P., and D. A. Goodenough. 1973. Fracture faces of zonulae occludentes from "tight" and "leaky" epithelia. *J. Cell Biol.* 58:390–400.

7. Coleman, T. R., and M. S. Mooseker. 1985. Effects of actin filament cross-linking and filament length of actin-myosin interaction. *J. Cell. Biol.* 101:1850–1857.

8. Dawson, D. C. 1977. Na and Cl transport across the isolated turtle colon: parallel pathways for transmural ion movement. *J. Membr. Biol.* 37:213–233.

9. Duffey, M. E., B. Hainau, S. Ho, and C. J. Bentzel. 1981. Regulation of epithelial tight junction permeability by cyclic AMP. *Nature (Lond.).* 204:451–453.

10. Flanagan, M. D., and S. Lin. 1980. Cytochalasins block actin filament elongation by binding to high affinity sites associated with F-actin. *J. Biol. Chem.* 225:835–838.

11. Freel, R. W., M. Hatch, D. L. Earnest, and A. M. Goldner. 1983. Role of tight-junctional pathways in bile salt-induced increases in colonic permeability. *Am. J. Physiol.* 8:G816–G824.

12. Frizzell, R. A., and S. G. Schultz. 1972. Ionic conductances of extracellular shunt pathway in rabbit ileum. Influence of shunt on transmural sodium transport and electrical potential differences. *J. Gen. Physiol.* 59:319–346.

13. Hirokawa, N., T. C. S. Keller, R. Chason, and M. S. Mooseker. 1983. Mechanism of brush border contractility studied by the quick-freeze deep-etch method. *J. Cell Biol.* 96:1325–1336.

14. Hirokawa, N., and L. G. Tilney. 1982. Interactions between actin filaments and between actin filaments and membranes in quick-frozen and deeply etched hair cells of the chick ear. *J. Cell Biol.* 95:249–261.

15. Hull, B. E., and L. A. Staehlin. 1979. The terminal web. A reevaluation of its structure and function. *J. Cell Biol.* 81:67–82.

16. Keller, T. C. S., K. A. Conzelman, R. Chason, and M. S. Mooseker. 1985. Role of myosin in terminal web contraction in isolated intestinal epithelial brush borders. *J. Cell Biol.* 100:1647–1655.

17. Keller, T. C. S., and M. S. Mooseker. Ca^{++}-calmodulin dependent phosphorylation of myosin, and its role in brush border contraction in vitro. *J. Cell Biol.* 95:943–959.

18. Lanman, R. C., J. A. Burton, and L. C. Schanker. 1971. Diffusion coefficients of some ^{14}C-labeled saccharides of biological interest. *Life. Sci.,* 10:803–811.

19. MacLean-Fletcher, S., and T. D. Pollard. 1980. Mechanism of action of cytochalasin B on actin. *Cell* 20:329–341.

20. Madara, J. L. 1983. Increases in guinea pig small intestinal transepithelial resistance induced by osmotic loads are accompanied by rapid alterations in absorptive-cell tight junction structure. *J. Cell Biol.,* 97:125–136.

21. Madara, J. L., and K. Dharmsathaphorn. 1985. Occluding junction structure–function relationships in a cultured epithelial monolayer. *J. Cell Biol.* 101:2124–2133.

22. Marcial, M. A., S. L. Carlson, and J. L. Madara. 1984. Partitioning of paracellular conductance along the ileal crypt-villus axis: a hypothesis based on structural analysis with detailed consideration of tight junction structure-function relationships. *J. Membr. Biol.* 80:59–70.

23. Meza, I., G. Ibarra, M. Sabenero, A. Martinez-Palomo, and M. Cereijido. 1980. Occluding junctions and cytoskeletal components in a cultured transporting epithelium. *J. Cell Biol.* 87:746–754.

24. Meza, I., M. Sabanero, E. Stefoni, and M. Cereijido. 1982. Occluding junctions in MDCK cells: modulation of transepithelial permeability by the

cytoskeleton. *J. Cell. Biochem.* 18:407–421.

25. Okada, Y., A. Irimajiri, and A. Inouye. 1977. Electrical properties and active solute transport in rat small intestine. II. Conductive properties of transepithelial routes. *J. Membr. Biol.* 31:221–232.

26. Owaribe, K., R. Kodama, and G. Eguchi. 1981. Demonstration of contractility of circumferential actin bundles and its morphogenic significance in pigmented epithelium in vitro and in vivo. *J. Cell Biol.* 90:507–514.

27. Palant, C. E., M. D. Duffey, B. K. Mookerjee, S. Ho, and C. J. Bentzel. 1983. Ca^{+2} regulation of tight-junction permeability and structure in Necturus gallbladder. *Am. J. Physiol.* 245:C203–C212.

28. Pitelka, D. R., and B. Taggart. 1983. Mechanical tension induces lateral movement of intramembrane components of the tight junction: studies on mouse mammary cells in culture. *J. Cell Biol.* 96:606–612.

29. Powell, D. W. 1981. Barrier function of epithelia. *Am. J. Physiol.* 241:6275–6288.

30. Rassat, J., H. Robenek, and H. Themann. 1982. Cytochalasin B affects the gap and tight junctions of mouse hepatocytes in vivo. *J. Submicrosc. Cytol.* 14:427–439.

31. Renkin, E. M., and F. E. Curry. 1979. Transport of water and solutes across capillary endothelium. *In* Membrane Transport in Biology. Transport Across Multimembrane Systems. Vol. IV A. G. Giebisch, D. C. Tosteson, and H. H Ussing, editors. Springer-Verlag, New York. 1–45.

32. Rodewald, R. S., S. B. Newman, and M. J. Karnovsky. 1976. Contraction of isolated brush borders from the intestinal epithelium. *J. Cell Biol.* 70:541–554.

33. Schliwa, M. 1982. Action of cytochalasin D on cytoskeleton networks. *J. Cell Biol.* 92:79–91.

34. Trier, J. S., and J. L. Madara. 1981. Functional morphology of the mucosa of the small intestine. *In* Physiology of the Gastrointestinal Tract. Vol. II. L. R. Johnson, editor. New York, Raven Press. 925–961.